ELSEVIER

Catalysis Today 78 (2003) 311–317

CATALYSIS TODAY

www.elsevier.com/locate/cattod

Defined vanadium phosphorus oxides and their use as highly effective catalysts in ammoxidation of methyl aromatics

Andreas Martin*, V. Narayana Kalevaru, Bernhard Lücke

Institut für Angewandte Chemie Berlin-Adlershof e.V., Richard-Willstätter-Str. 12, D-12489 Berlin, Germany

Abstract

The heterogeneous catalytic ammoxidation of methyl aromatics and methyl hetero aromatics is a preferred method for the synthesis of aromatic and hetero aromatic nitriles. The resulting nitriles are valuable intermediates for the production of dyestuffs, pesticides, pharmaceuticals and other chemical products. Usually, the ammoxidation is carried out using V-containing oxides (e.g. V/Ti, V/Sn, V/Mo) promoted by further transition metals as catalysts. However, we have shown recently that defined vanadium phosphates (VPO) revealed an excellent ammoxidation performance. The ammoxidation of toluene was used as model reaction. An intense characterisation of some VPO catalysts under pre-treatment and working conditions by the use of various in situ-methods has thrown more light in formation and stability of the used VPO solids as well as the effect of different reactants (ammonia, toluene) on VPO surface and bulk properties.

Keywords: Ammoxidation; Vanadium phosphorus oxide catalysts; Substituted methyl aromatics; Nitriles; In situ-techniques

1. Introduction

Vanadium phosphates (VPO) of different structure and vanadium valence state are suitable precursor compounds of very active and selective catalysts for the ammoxidation of various methyl aromatic (e.g. toluene, xylenes, halotoluenes, etc.) as well as hetero aromatic reactants (e.g. picolines, methylpyrazines, etc.) [1–4]. The ammoxidation of those reactants enables an economic and ecologic route to valuable intermediates in organic syntheses of different dyestuffs, pharmaceuticals and pesticides and, hence, it is indeed an industrially important reaction (e.g. [4,5]). Detailed reports on the catalytic performance of VPO catalysts in ammoxidation of methyl aromatics and methyl hetero aromatics are given elsewhere [2,4].

Recently, we have found out the formation of $(NH_4)_2(VO)_3(P_2O_7)_2$ as XRD-detectable phase when $VOHPO_4{\cdot}xH_2O$ ($x = 0$, 1/2, 2 and 4) is heated in the presence of ammonia, air and water vapour [6]; caused by the stoichiometry of the transformation reaction (from $V/P = 1 \Rightarrow V/P = 0.75$) and the determination of the vanadium oxidation state of the transformation product (≈4.11 [6]) clearly indicates that a second, mixed-valent (V^{IV}/V^{V}) vanadium-rich phase (V_xO_y) must be formed in addition to $(NH_4)_2(VO)_3(P_2O_7)_2$. The V_xO_y phase seems to be primarily responsible for the catalytic activity and an increase in its proportion could boost the catalyst performance considerably.

In situ-methods are well known as powerful tools in studying catalyst formation processes, their solid-state properties under working conditions and the interaction with the reactants, intermediates and products to establish reaction mechanisms (e.g. [7]). This paper

* Corresponding author. Tel.: +49-30-63924306.
E-mail address: a.martin@aca-berlin.de (A. Martin).

0920-5861/02/$ – see front matter
PII: S0920-5861(02)00312-7

gives a short overview on results of intense studies using in situ-techniques to reveal VPO catalyst generation processes, interaction of educts, intermediates and products with VPO catalyst surfaces and some mechanistic insights. Catalytic data of the ammoxidation of toluene on different VPOs complete these findings. The precursor–catalyst transformation processes were investigated by in situ-XRD, in situ-Raman and in situ-ESR spectroscopy. The interaction of toluene used as a model compound with VPO solids was recorded by in situ-ESR and in situ-FTIR spectroscopy. Mechanistic information was mainly obtained using in situ-FTIR spectroscopy and the temporal-analysis-of-products (TAP) technique. Catalytic studies were carried out in a fixed-bed microreactor on pure $(NH_4)_2(VO)_3(P_2O_7)_2$, generated $[(NH_4)_2(VO)_3(P_2O_7)_2 + V_xO_y]$ catalysts, having different V_xO_y proportions by use of $VOHPO_4{\cdot}(1/2)H_2O$ (V/P = 1) and $(VO)_3(PO_4)_2{\cdot}7H_2O$ (V/P = 1.5) precursors; the well-known $(VO)_2P_2O_7$ was used for comparison.

2. Experimental

The precursor compounds $VOHPO_4{\cdot}(1/2)H_2O$ ($VP_{(1/2)H}$) and $(VO)_3(PO_4)_2{\cdot}7H_2O$ (VP_{7H}) have been prepared in aqueous solutions as described elsewhere [8]. The materials were pressed and crushed (1–1.25 mm) and then pre-treated by heating to 673 K under NH_3:air:H_2O vapour (molar ratio = 1:7:5, total flow = 13 l h^{-1}) for 5 h. The catalyst materials are denoted as $AVP_{gen(1/2)H}$ and AVP_{gen7H}, respectively. The as-synthesised solids contain different proportions of the mixed-valent V_xO_y phase (see Eqs. (1) and (2), Table 1). Pure $(NH_4)_2(VO)_3(P_2O_7)_2$ (AVP_{syn}) has been synthesised according to the procedure by Zhang et al. [6]. Pure $(VO)_2P_2O_7$ solid (VPP) that has been generated by usual dehydration of $VP_{(1/2)H}$ precursor is applied as model catalyst for comparison

$$4V^{IV}OHPO_4 \cdot \tfrac{1}{2}H_2O(2NH_3, O_2) \Rightarrow [(NH_4)_2(V^{IV}O)_3(P_2O_7)_2 + V_x^{IV/V}O_y] + 3H_2O \quad (1)$$

$$2(V^{IV}O)_3(PO_4)_2 \cdot 7H_2O(2NH_3, O_2) \Rightarrow [(NH_4)_2(V^{IV}O)_3(P_2O_7)_2 + 3V_x^{IV/V}O_y] + 13H_2O \quad (2)$$

The precursor–catalyst transformation was followed by in situ-XRD using a commercial reactor chamber (A. Paar, Austria) that could be heated up to 1173 K (sample amount ca. 150 mg) [9]. The reactor chamber is coupled with an on-line capillary GC to check catalytic properties during transformation. Similar studies were carried out in a homemade water cooled in situ-Raman cell ($T < 873$ K, sample amount ca. 10–20 mg, 2.5 mW power level) [10]. The cell is mounted on a DILOR-XY spectrometer (Ar-laser, backscatter geometry, micro-Raman technique). ESR measurements were performed with the cw spectrometer ERS 300 (ZWG) equipped for in situ-investigations with a flow reactor (400 mg catalyst) and a gas as well as liquids metering system (e.g. [11]). The infrared spectra were recorded with a Bruker IFS 66 FTIR spectrophotometer using self-supporting discs mounted in an in situ-cell connected with a gas manifold-evacuation system. A TAP reactor unit was used for the investigation of the effect of a prereduction–preoxidation of a VPO catalyst near-surface region on its catalytic properties [12] and for isotope experiments ($^{15}NH_3$-containing feed) [13] to study the role of NH_4^+ ions during the catalytic cycle.

The catalytic properties of the solids were determined during the ammoxidation of toluene to benzonitrile using a fixed-bed U-tube quartz-glass reactor (ca. 1.5 g catalyst). The following reaction conditions were applied—toluene:NH_3:air:H_2O

Table 1
Chemical analyses, BET surface areas and vanadium valence states of the solids used for further characterisation and ammoxidation runs

Samples	N (wt.%)	H (wt.%)	H/N molar ratio	V (wt.%)	BET surface area ($m^2\,g^{-1}$)	V valence state
AVP_{syn}	4.77	1.37	4.02	25.91	3.04	4.000
$AVP_{gen(1/2)H}$	4.95	1.28	3.62	29.17	2.95	4.111
AVP_{gen7H}	3.81	0.95	3.49	35.24	3.60	4.248
VPP	–	–	–	32.83	5.31	4.007

vapour = 1:4.5:32:24, atmospheric pressure, W/F = ca. 10 g h mol^{-1} (total flow). The catalytic runs were performed at ca. 573, 598 and 623 K for 45 min each. Toluene conversion and benzonitrile yield were followed by on-line capillary GC using an FID as detector.

3. Results and discussion

Fig. 1 depicts the in situ-XRD patterns obtained during heating the $VP_{(1/2)H}$ precursor up to 713 K under NH_3-containing feed. The transformation proceeds via dehydration, incorporation of NH_4^+ ions and formation of the three-dimensional AVP structure [6]. The transformation process is finished after ca. 4–5 h. Cooling under N_2 reveals the pattern of pure AVP, i.e. no additional information on a V_xO_y phase could be obtained. Otherwise, cooling down the sample under the NH_3-containing feed (up to 393 K) generates NH_4VO_3 particles besides AVP as clearly identified by the obtained patterns as shown in Fig. 2(a). The lines indicate the NH_4VO_3 reflections. For comparison, the pattern of pure AVP_{syn} is shown in Fig. 2(b). Thus, it

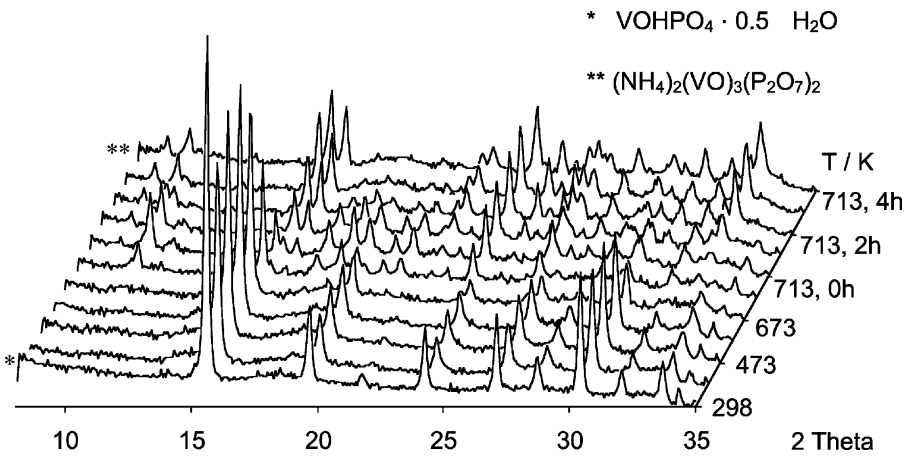

Fig. 1. In situ-XRD patterns of the $VOHPO_4 \cdot (1/2)H_2O$ phase transformation into $(NH_4)_2(VO)_3(P_2O_7)_2 + V_xO_y$ ($AVP_{gen(1/2)H}$) [9].

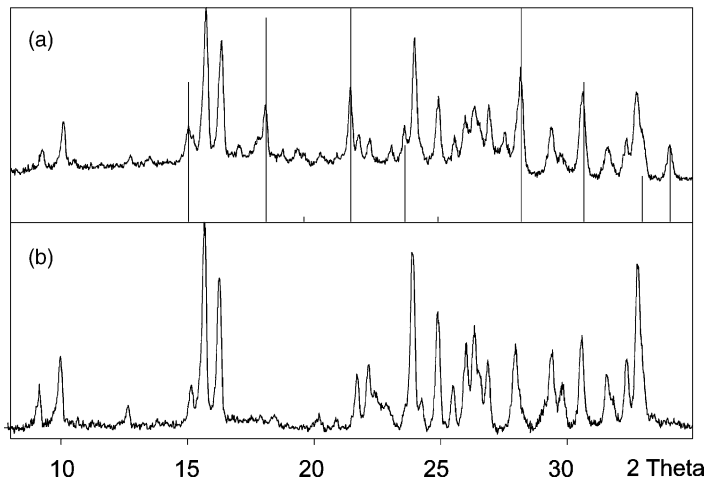

Fig. 2. XRD patterns of the $(NH_4)_2(VO)_3(P_2O_7)_2 + V_xO_y$ catalyst ($AVP_{gen(1/2)H}$) obtained after cooling under NH_3-containing feed (NH_4VO_3 marked by lines) (a) in comparison to pure $(NH_4)_2(VO)_3(P_2O_7)_2$ (AVP_{syn}) (b).

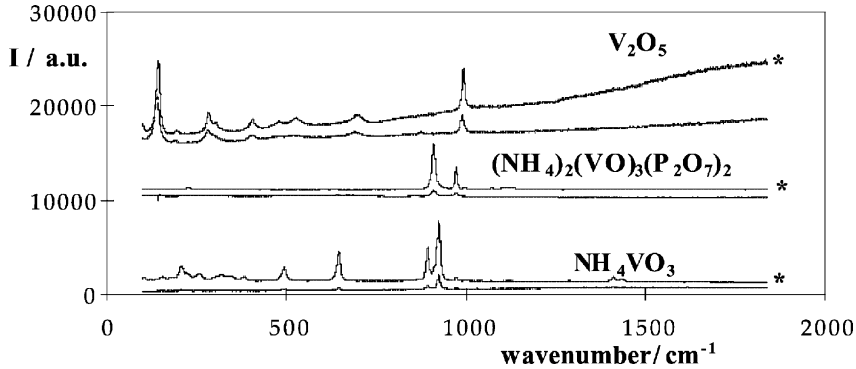

Fig. 3. Raman spectra of selected surface areas (micro-Raman technique) of an $(NH_4)_2(VO)_3(P_2O_7)_2 + V_xO_y$ catalyst ($AVP_{gen(1/2)H}$) obtained after phase transformation in comparison to spectra of pure compounds (marked by ∗).

seems very likely that NH_4VO_3 could be formed from mixed-valent vanadium oxides, existing under reaction conditions and an excess of closely neighboured NH_4^+ ions [6]. The transformation of the orthophosphate precursor VP_{7H} proceeds in a similar manner, but various, more intense reflections in the pattern of the N_2 cooled transformation product point to different vanadium oxides however, a specific assignment to define solids is not observable.

Recently, the $VP_{(1/2)H}$ transformation process into $AVP_{gen(1/2)H}$ was also followed by in situ-Raman spectroscopy. The Raman spectra revealed the existence of NH_4VO_3 [10]. Moreover, it was possible to find areas that consist of V_2O_5 mainly. NH_4VO_3 and V_2O_5 are spatially separated from the AVP surface as detected by the micro-Raman technique [10].

Fig. 3 presents Raman spectra of selected surface areas (marked by ∗) using an Olympus 10× objective (laser focus ca. 10 μm) in comparison to the pure solids. The search for lower-valent vanadium oxides was not successful because V^{IV}-containing vanadium oxides are not so easy to detect by Raman spectroscopy. This fact is strengthened by the simultaneous presence of V^V compounds as in this case.

In situ-ESR spectroscopy can be applied as a useful tool for the characterisation of the electronic properties of V^{IV}-containing solids and their interaction with feed components during catalytic runs [11]. Fig. 4 shows in situ-ESR spectra of the $VP_{(1/2)H}$ transformation and the respective quotients of the fourth and the square of the second moment of the ESR signals, characterising the efficiency of the spin–spin exchange between neighbouring VO^{2+} ions. The spectra reveal that the transformation proceeds via a strongly disordered state. The exchange efficiency is also related to the catalytic activity (e.g. [12]). Active catalysts contain coupled vanadyl sites and are characterised by a high degree of the exchange efficiency in comparison to less active ones with mostly isolated vanadyl centres. The reason therefore could be that the alteration of the electron density at a discrete surface vanadyl unit caused by the redox process can easily be delocalised via the overlapping d-orbitals of the exchange coupled sites [14]. These moment quotients spin–spin exchange values also change during interaction of the solid with feed components. For example, in situ-studies revealed that substituted toluenes with electron-donating substituents (e.g. $–OCH_3$) disturb the spin–spin exchange much more than toluene or educts having rather electron-withdrawing groups (e.g. –Cl) [15]. This is due to a stronger interaction of the more basic ring systems with the vanadyl sites of the surface. These findings are reflected in catalytic runs under comparable conditions; conversion and nitrile selectivity are decreased in the $–OCH_3$ case compared to the reaction of Cl-toluenes (e.g. [2]).

In situ-ESR and in situ-FTIR spectroscopic studies [16] also confirm the reaction mechanism of the ammoxidation of toluene on VPO catalysts that showed coupled vanadyl sites as in the case of $(VO)_2P_2O_7$ (Fig. 5). These ideas could also be transferred to vanadium oxide surfaces. Some V–O–V and/or V–O–P links are hydrated under reaction conditions and NH_4^+ ions are formed. The toluene molecule is chemisorbed

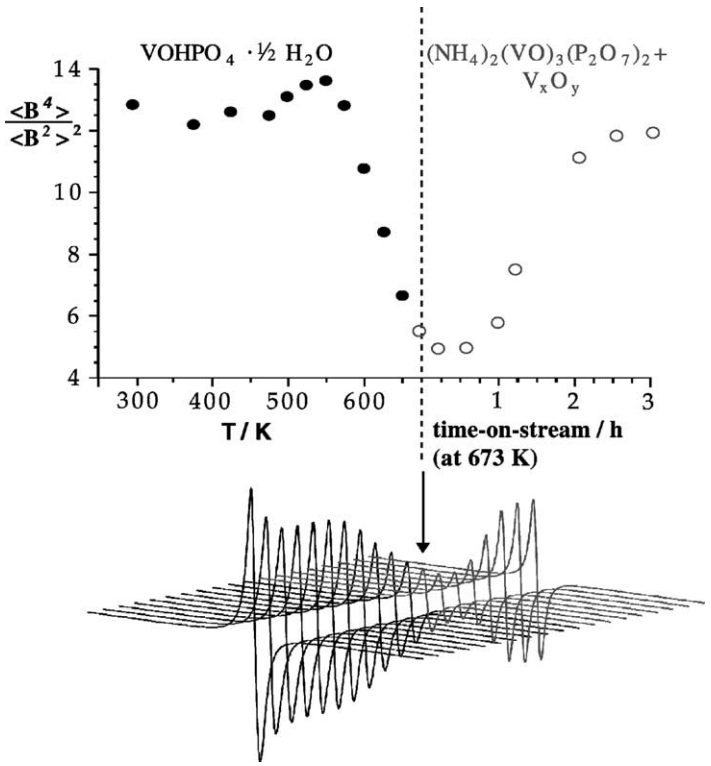

Fig. 4. In situ-ESR spectra of the $VOHPO_4{\cdot}(1/2)H_2O$ transformation into $(NH_4)_2(VO)_3(P_2O_7)_2 + V_xO_y$ ($AVP_{gen(1/2)H}$).

on a Lewis-acid vanadyl site; the reaction proceeds via methylene species, benzaldehyde, benzylimine to benzonitrile as indicated by in situ-FTIR spectroscopy.

Pulse catalytic experiments using the TAP technique, $(VO)_2P_2O_7$ as catalyst and toluene as educt revealed a distinct dependence of the catalytic activity and product selectivity on the oxidation state of the catalyst surface [12]. The catalyst surface was oxidised by O_2 and reduced by NH_3 pulses. The investigations showed that an increasing proportion of surface V^V accelerates the catalytic process but the nitrile selectivity drops by over-oxidation, otherwise, increasing surface V^{III} portions drastically restricts the catalytic activity.

Some TAP followed ammoxidation runs were also carried out on AVP_{syn} to study the role of NH_4^+ ions during ammoxidation using $^{15}NH_3$-containing feed [13]. The experiments revealed that no gas phase ammonia reacts and NH_4^+ ions participate as potential nitrogen source in the nitrile formation. It was found out that during an ammoxidation pulse series only ^{14}N-benzonitrile is formed at first and the portion of ^{15}N-benzonitrile slowly increases with further pulses. It seems very likely that the NH_4^+ ions formed during catalytic runs could be able to intervene in the mechanism as well. Fig. 6 schematically depicts these ideas.

Fig. 7 demonstrates area-specific toluene conversion rates of different AVP catalysts and the usual VPP specimen, depending on the reaction temperature. Pure AVP_{syn} (exposing single vanadyl sites on the surface) seems to be nearly inactive. The conversion rate of the VPP catalyst (edge-shared vanadyl dioctahedra units) looks rather low as well. Owing to the existence of mixed-valent V_xO_y (planes of edge-shared vanadyl octahedra) of the AVP_{gen} solids and additionally in increased portions of the orthophosphate derived catalyst, these solids reveal a significant enhancement of the toluene conversion rate at almost equal high nitrile selectivities in comparison to the other VPOs.

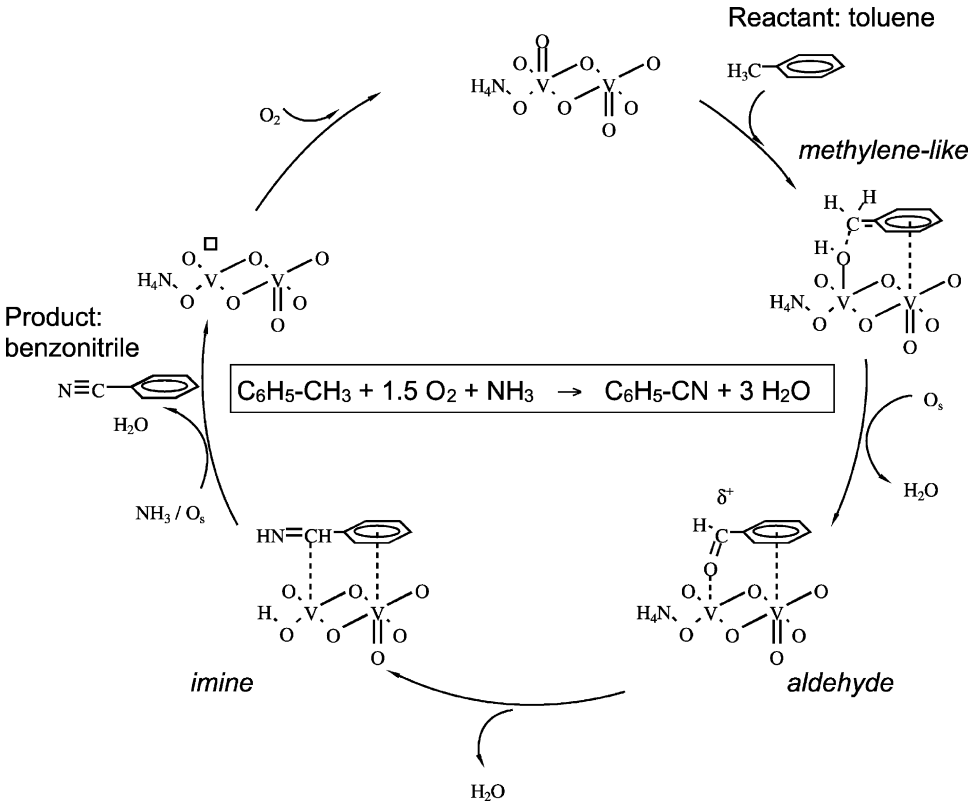

Fig. 5. Reaction mechanism of the toluene ammoxidation on a vanadyl dioctahedra unit (100 plane) of $(VO)_2P_2O_7$ [16].

In conclusion, the studies have shown that in situ-methods could help to reveal and understand catalyst formation processes and the effect of catalyst–feed interaction on conversion of reactant and selectivity of desired products. It could be seen that an active and selective ammoxidation on VPOs requires (i) adjacent vanadyl units, (ii) an easy and fast change of the surface V-valence that should be +4 on the average and

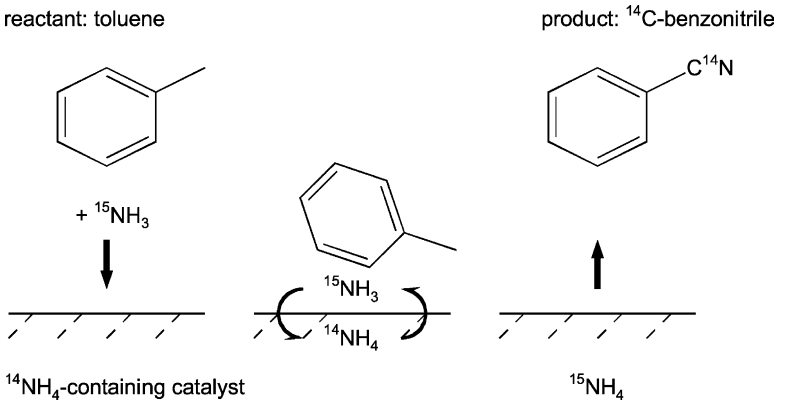

Fig. 6. N-insertion during ammoxidation by NH_4^+ ions of the solid.

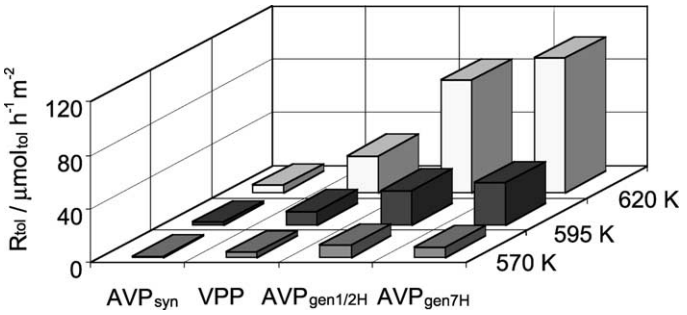

Fig. 7. Area-specific rate of toluene conversion during ammoxidation runs using NH_4^+-containing VPO catalysts and $(VO)_2P_2O_7$ (VPP) for comparison.

(iii) the presence of NH_4^+ as structural unit or rapidly generated by hydrolysis of V–O–P links.

Acknowledgements

The authors thank Drs. Brückner, Bentrup, Wilde, Witke (BAM) and Zhang for their experimental help and fruitful discussions.

References

[1] A. Martin, B. Lücke, H. Seeboth, G. Ladwig, E. Fischer, React. Kinet. Catal. Lett. 38 (1989) 33.
[2] A. Martin, B. Lücke, Catal. Today 32 (1996) 279.
[3] I. Matsuura, Stud. Surf. Sci. Catal. 72 (1992) 247.
[4] A. Martin, B. Lücke, Catal. Today 57 (2000) 61.
[5] R.G. Rizayev, E.A. Mamedov, V.P. Vislovskii, V.E. Sheinin, Appl. Catal. A 83 (1992) 103.
[6] Y. Zhang, A. Martin, G.-U. Wolf, S. Rabe, H. Worzala, B. Lücke, M. Meisel, K. Witke, Chem. Mater. 8 (1996) 1135.
[7] M. Hunger, J. Weitkamp, Angew. Chem. 113 (2001) 3040.
[8] A. Martin, G.-U. Wolf, U. Steinike, B. Lücke, J. Chem. Soc., Faraday Trans. 94 (1998) 2227.
[9] A. Martin, L. Wilde, U. Steinike, J. Mater. Chem. 10 (2000) 2368.
[10] Y. Zhang, M. Meisel, A. Martin, B. Lücke, K. Witke, K.-W. Brzezinka, Chem. Mater. 9 (1997) 1086.
[11] A. Brückner, B. Kubias, B. Lücke, Catal. Today 32 (1996) 215.
[12] A. Martin, Y. Zhang, M. Meisel, React. Kinet. Catal. Lett. 60 (1997) 3.
[13] A. Martin, Y. Zhang, H.W. Zanthoff, M. Meisel, M. Baerns, Appl. Catal. A 139 (1996) L11.
[14] A. Brückner, A. Martin, N. Steinfeldt, G.-U. Wolf, B. Lücke, J. Chem. Soc., Faraday Trans. 92 (1996) 4257.
[15] A. Brückner, A. Martin, B. Lücke, F.K. Hannour, Stud. Surf. Sci. Catal. 110 (1997) 919.
[16] Y. Zhang, A. Martin, H. Berndt, B. Lücke, M. Meisel, J. Mol. Catal. A 118 (1997) 205.